JOURNAL OF GUIDANCE, CONTROL, AND DYNAMICS
Vol. 20, No. 3, May–June 1997

Engineering Notes

ENGINEERING NOTES are short manuscripts describing new developments or important results of a preliminary nature. These Notes cannot exceed 6 manuscript pages and 3 figures; a page of text may be substituted for a figure and vice versa. After informal review by the editors, they may be published within a few months of the date of receipt. Style requirements are the same as for regular contributions (see inside back cover).

Suboptimal Singular Orbital Transfer

I. Michael Ross*
U.S. Naval Postgraduate School, Monterey, California 93943

Introduction

IN the fuel optimization of space trajectories, it is well known that the totality of optimal thrust arcs consists of the null thrust arc, a singular thrust arc, and the maximum thrust arc.[1] If we limit ourselves to piecewise continuous functions, the singular thrust arcs are intermediate thrust arcs and allow the possibility of thrust modulation, the most well known of these being the Lawden's spiral.[1] In most cases, the intermediate thrust arcs are not optimal because of their failure to satisfy higher-order necessary conditions such as the generalized Legendre–Clebsch condition (GLC). Hence, in the determination of optimal space trajectories, one can formulate a nonlinear version of the bang-bang principle, and what remains to be determined for a given problem is the number of burns and the switching structure. This is the standard problem.

The singular arcs discussed in the literature for exoatmospheric space flight are of order two. They are also partially singular because only the thrust magnitude is singular while the steering is regular; in fact, it is aligned with the primer vector. In many practical cases, it may be more convenient to steer the vehicle differently than the primer. Two classic examples of such guidance methods are geocentric and inertial steering.[2] Recent research[3,4] indicates that if the steering is not optimal but prescribed a priori by, say, a state feedback law, then the resulting singular arc is dramatically modified. For example, because steering is no longer a control vector, it renders the problem totally singular. These steering-induced singular arcs potentially satisfy the GLC and are of order one. Satisfaction of the convexity condition makes these arcs a strong candidate for an optimal subarc while the reduction in order renders them more favorable to joining with a regular subarc vis-á-vis the McDanell–Powers junction conditions.[5]

When the steering is tangential (i.e., parallel to the velocity vector), it yields an astonishingly simple singular arc whose thrust program T_s is given by[3,4]

$$T_s = mg \sin \gamma \tag{1}$$

where m is the mass of the spacecraft; $g = \mu / r^2$, where μ is the gravitational constant; and r and γ are the radial position and flight-path angle, respectively. It is clear that (see Fig. 1) the singular thrust is simply equal to a component of the gravitational force. In this Note, we further describe this singular burn by deriving additional integrals of motion. The new integrals are used to derive the controllable domain from which a circular orbit may be targeted by singular thrusting. We also show that the singular thrust may be interpreted as complementary to the impulsive burn. The results are applied to the problem of transferring a spacecraft from an initial elliptical orbit to a final nonintersecting circular orbit.

Further Analysis of the Singular Trajectory

The equations of motion along and perpendicular to the velocity are

$$\dot{v} = (T/m) - g \sin \gamma \tag{2a}$$

$$\dot{\gamma} = [(v^2/r) - g](\cos \gamma / v) \tag{2b}$$

where v is the speed of the spacecraft. Clearly, over a singular thrust arc, we have

$$v = \text{const} \tag{3}$$

An additional integral of motion can now be obtained by using this result and the kinematical relationship

$$\dot{r} = v \sin \gamma \tag{4}$$

as follows. Dividing Eq. (4) by Eq. (2b), we have

$$\frac{\mathrm{d}r}{\mathrm{d}\gamma} = \frac{v^2 \sin \gamma / \cos \gamma}{v^2/r - \mu / r^2} \tag{5}$$

which is a separable differential equation because we can rewrite it as

$$\int \left(\frac{v^2}{r} - \frac{\mu}{r^2} \right) \mathrm{d}r = -v^2 \int \frac{\mathrm{d}(\cos \gamma)}{\cos \gamma} \tag{6}$$

to yield

$$v^2 \ln r + (\mu / r) = -v^2 \ln \cos \gamma + A \tag{7}$$

where A is a constant of integration that yields a family of singular trajectories. This simplifies to

$$v^2 \ln (r \cos \gamma) + (\mu / r) = A \tag{8}$$

The preceding equation can be written more succintly in terms of the angular momentum, $h = rv \cos \gamma$, as

$$\ln (h / h_0) = (\mu / v^2)[(1/r_0) - (1/r)] \tag{9}$$

where (r_0, h_0) is a point on the singular arc. In deriving this equation, we have used the fact that $v = \text{const}$. Thus, a singular burn rotates the velocity vector while raising the orbit. From an energy point of view, singular thrusting affects only the potential energy,

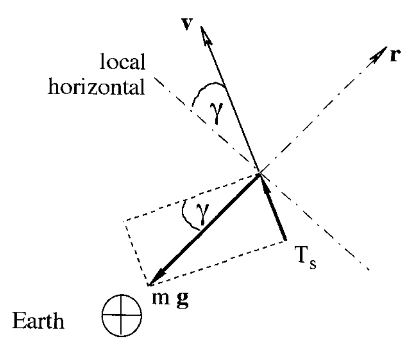

Fig. 1 Singular thrust program, $T_s = mgs\gamma$.

Received Dec. 6, 1996; revision received Feb. 5, 1997; accepted for publication Feb. 19, 1997. This paper is declared a work of the U.S. Government and is not subject to copyright protection in the United States.

*Assistant Professor, Department of Aeronautics and Astronautics, Mail Code AA-Ro. E-mail: ross@aa.nps.navy.mil. Senior Member AIAA.

leaving the kinetic energy intact. In this sense, it may be viewed as complementary to the impulsive delta-V maneuver that affects only the kinetic energy leaving the potential energy intact. An exact equation relating the change in the potential energy to the propellant consumption may be obtained by substituting $T = T_s$ in the rocket equation,

$$\dot{m} = -\frac{T}{v_e} = -\frac{mg\sin\gamma}{v_e} \tag{10}$$

where v_e is the rocket exhaust speed. Combining this with Eq. (4), we arrive at a separable differential equation,

$$\dot{m} = -\frac{m\mu\dot{r}}{r^2 v_e v} \tag{11}$$

that integrates to

$$\ln(m) = (\mu/v_e v)[(1/r) + B] \tag{12}$$

where B is a constant of integration. If we let (r_0, m_0) be a point on the singular arc, then we can rewrite the preceding equation as

$$\ln(m_0/m) = (\mu/v_e v)[(1/r_0) - (1/r)] \tag{13}$$

or in terms of the characteristic velocity c,

$$c = v_e \ln(m_0/m) = (\mu/v)[(1/r_0) - (1/r)] \tag{14}$$

Targeting a Circular Orbit

If a circular orbit can be reached by a singular trajectory, then the following conditions must be met:

$$v_0 = v_f \tag{15a}$$

$$A = v_f^2 \ln(r_f) + (\mu/r_f) \tag{15b}$$

where the subscripts 0 and f denote initial and final conditions, respectively. Equations (8) and (15) yield a compact condition for a point on the initial elliptic orbit in terms of the flight-path angle given by

$$\cos\gamma_0 = \frac{\exp(1 - 1/k^2)}{k^2} \tag{16}$$

where k is the Kepler number, defined as the ratio of the initial speed to the local circular speed,

$$k = v_0/v_c \qquad v_c = \sqrt{\mu/r_0} \tag{17}$$

Note that we must have $k < 1$ to perform this maneuver (because $v = \text{const}$ and the orbit is being raised). The controllable states, and hence the initial elliptic orbit, from which a circular target orbit can be reached by a singular burn can be parameterized by the Kepler number. Because

$$r_0 = k^2 r_f \tag{18}$$

Equations (15a), (16), and (18) determine a unique point on the initial orbit [because $\gamma_0 > 0$; cf. Eq. (1)] whose orbital parameters follow from standard conic equations. Thus, if the initial and final orbits meet these conditions, a singular transfer orbit can be designed. Using the results of Ref. 3, it can be shown that for the time-free problem this totally singular transfer orbit is not fuel optimal due to its failure to satisfy the terminal transversality conditions. However, this does not eliminate the singular arc as a potential candidate for optimality under a different switching structure that terminates with a nonsingular burn. Further, the nonoptimality does not necessarily hold for the time-fixed problem. Compounding this complication is the fact that the maximum principle provides only a binary test on the optimality of a given trajectory. That is, the necessary conditions do not indicate whether or not a given trajectory, if nonoptimal, is close to the optimal. Here, we use the word close in the sense of the performance index. One way to handle these theoretical drawbacks is to resort to numerical analysis. Lawden's recent numerical study[6] shows that, although his second-order singular arc is nonoptimal, it is generally within 1% of the cost of the best two-impulsive maneuver.

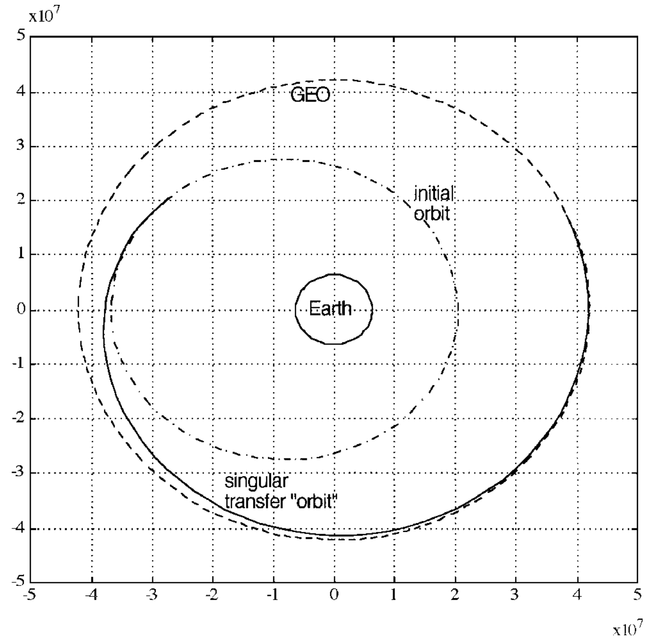

Fig. 2 Transfer orbit by a singular burn; ordinate and abscissa are in meters.

Motivated by this analysis, we numerically investigate the problem of transferring a spacecraft by a singular burn and compare it to a two-impulse maneuver.

Numerical Example

Consider the problem of transferring a spacecraft from an initial elliptical orbit given by $a = 28{,}700$ km and $e = 0.2846$ to a coplanar geosynchronous orbit given by $a = 42{,}164$ km and $e = 0$. The initial orbit parameters are chosen so that a totally singular orbit transfer is a feasible maneuver. The two-impulse Hohman type maneuver consists of a delta-V at the perigee of the initial orbit followed by a circularization delta-V at geosynchronous Earth orbit (GEO). The characteristic velocity for this maneuver is 702.5 m/s. A singular orbit transfer is a continuous burn starting at that point on the initial orbit where the speed is equal to 3075 m/s and ending at GEO (see Fig. 2). This point is $\theta = 143.15$ deg, where θ is the true anomaly. The characteristic velocity for this maneuver is 721.2 m/s. Obviously, the impulsive maneuver is more efficient. However, the difference in the characteristic velocity is only 18.7 m/s (or equivalently about 2.7%). Clearly, it is more suboptimal than nonoptimal. A different switching structure, one that does not terminate with a singular arc, holds the potential for reducing the characteristic velocity. Further, if the performance measure were to include the transfer time, it is apparent (see Fig. 2) that a singular burn might be a subarc, for example, a singular arc that does not target a circular orbit followed by an impulsive burn at GEO to complete the rotation of the velocity. That analysis is beyond the scope of this Note but is a subject of current research.

Conclusions

Singular arcs arising in the optimization of space trajectories were previously thought to be of order two. When the steering is prescribed a priori, it yields new singular arcs that are of order one. The analysis of one such first-order singular arc shows that it may be used to design suboptimal orbit transfers. A time-fixed optimal maneuver might contain a singular subarc. A detailed analysis of these steering-induced singular arcs is necessary to fully explore alternative mission designs.

Acknowledgments

This research was supported by the Naval Postgraduate School and the Air Force Space Command (AFSC). I would like to express my special gratitude to Brian D. Neuenfeldt at AFSC for sponsoring this research and to Kyle T. Alfriend for stimulating discussions on this topic.

References

[1]Marec, J. P., *Optimal Space Trajectories*, Elsevier Scientific, Amsterdam, 1979.

[2]Zondervan, K. P., and Sturgeon, S. D., "An Analytic Method for Determining Finite Burn Effects," AAS/AIAA Spaceflight Mechanics Meeting, AAS Paper 92-131, Colorado Springs, CO, Feb. 1992.

[3]Ross, I. M., "An Analysis of First-Order Singular Thrust-Arcs in Rocket Trajectory Optimization," *Acta Astronautica*, Vol. 39, No. 6, 1996, pp. 417–422.

[4]Ross, I. M., and Alfriend, K. T., "Low-Earth-Orbit Maintenance: Reboost Versus Thrust-Drag Cancellation," *Journal of Guidance, Control, and Dynamics*, Vol. 18, No. 4, 1995, pp. 930–932.

[5]McDanell, J. P., and Powers, N. F., "Necessary Conditions for Joining Optimal Singular and Nonsingular Subarcs," *SIAM Journal of Control*, Vol. 9, May 1971, pp. 161–173.

[6]Lawden, D. F., "Calculation of Singular Extremal Rocket Trajectories," *Journal of Guidance, Control, and Dynamics*, Vol. 15, No. 6, 1992, pp. 1361–1365.

Low-Thrust Orbit Raising with Coupled Plane Change and J_2 Precession

Colin R. McInnes*

University of Glasgow,

Glasgow G12 8QQ, Scotland, United Kingdom

I. Introduction

MANY compact analytical expressions currently exist to describe the orbit evolution of low-thrust transfer vehicles. These expressions are particularly useful for preliminary analysis of both vehicle and mission-design concepts. In particular, compact expressions exist for both orbit radius[1,2] and polar angle,[2] along with the well-known Edelbaum solutions[3] for Δv costs during optimal transfer. These solutions have also been extended by Wiesel and Alfano.[4]

Many low-thrust transfer vehicle applications center on payload orbit raising.[5,6] For solar-electric vehicles, eclipse conditions are clearly of importance. Therefore, nodal precession is important during preliminary mission design. In addition, other applications of low-thrust transfer vehicles for polar satellite servicing[7] require the vehicle to align the nodes of its orbit with the target satellite. Again, nodal precession is clearly of significant importance for such applications.

The dynamics of a low-thrust orbital transfer vehicle are considered under the action of nodal precession caused by Earth oblateness. The vehicle also generates an out-of-plane acceleration to continuously change the orbit inclination during the transfer maneuver. Because both the transfer vehicle semimajor axis and inclination are changing, the oblateness-induced nodal precession will be strongly coupled to the orbit evolution of the low-thrust vehicle. Therefore, a set of coupled, variational equations are derived, which may be averaged to obtain the long-term evolution of the low-thrust vehicle orbit with both nodal precession and thrust-induced accelerations. The resulting coupled equations may then be solved sequentially to obtain approximate analytic solutions for semimajor axis, true anomaly, inclination, and ascending node angle, thus compactly describing the orbit evolution of the low-thrust vehicle.

II. Vehicle Dynamics

For a low-thrust-to-weight ratio vehicle with a high-specific-impulse propulsion system, the reduction in vehicle mass due to propellant depletion may be neglected. Therefore, the transfer vehicle will be modeled with a constant, thrust-induced acceleration ε.

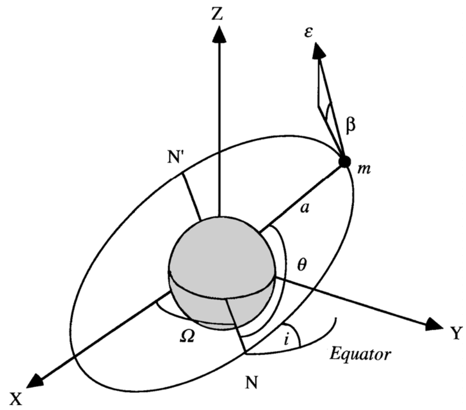

Fig. 1 Schematic orbit geometry with ascending node N and descending node N'.

This acceleration is directed along the vehicle velocity vector, but is pitched at an angle β relative to the orbit plane (Fig. 1). Again, assuming a low-thrust-to-weight ratio vehicle, the outward spiral is quasicircular. The orbit radius may then be replaced by the semimajor axis under the assumption that the orbit eccentricity is negligible. Under these conditions the Lagrange–Gauss variational equations[8] become

$$\frac{\mathrm{d}a}{\mathrm{d}t} = \frac{2\varepsilon}{\sqrt{\mu}} \cos\beta a^{\frac{3}{2}} \tag{1a}$$

$$\frac{\mathrm{d}\theta}{\mathrm{d}t} = \sqrt{\frac{\mu}{a^3}} \tag{1b}$$

$$\frac{\mathrm{d}\Omega}{\mathrm{d}t} = \varepsilon \sin\beta \sqrt{\frac{a}{\mu}} \frac{\sin\theta}{\sin i} - \frac{3}{2}\frac{\bar{n} J_2 R^2 \cos i}{a^2}$$
$$\bar{n} = \sqrt{\frac{\mu}{a^3}} + \mathcal{O}(J_2) \tag{1c}$$

$$\frac{\mathrm{d}i}{\mathrm{d}t} = \varepsilon \sin\beta \sqrt{\frac{a}{\mu}} \cos\theta \tag{1d}$$

where a represents the semimajor axis, θ the true anomaly, Ω the ascending node, i the orbit inclination, and μ the gravitational parameter. In addition, R represents the radius of the Earth and J_2 the oblateness parameter. It can be seen that Eq. (1c) contains both Earth oblateness- and thrust-induced precessions.

These equations may now be averaged with respect to true anomaly to obtain the long-period motion using the averaging operator

$$\langle z \rangle = \frac{1}{2\pi} \int_0^{2\pi} z \,\mathrm{d}\theta \tag{2}$$

Assuming that the out-of-plane thrust angle β is a function of true anomaly only and the change in elements during each orbit is small, the averaging operator may be applied to Eqs. (1) to yield

$$\left\langle \frac{\mathrm{d}a}{\mathrm{d}t} \right\rangle = \frac{\varepsilon}{\pi\sqrt{\mu}} a^{\frac{3}{2}} \int_0^{2\pi} \cos\beta(\theta)\,\mathrm{d}\theta \tag{3a}$$

$$\left\langle \frac{\mathrm{d}\theta}{\mathrm{d}t} \right\rangle = \sqrt{\frac{\mu}{a^3}} \tag{3b}$$

$$\left\langle \frac{\mathrm{d}\Omega}{\mathrm{d}t} \right\rangle = \frac{\varepsilon}{2\pi \sin i} \sqrt{\frac{a}{\mu}} \int_0^{2\pi} \sin\theta \sin\beta(\theta)\,\mathrm{d}\theta - \frac{3}{2}\frac{\sqrt{\mu} J_2 R^2 \cos i}{a^{\frac{7}{2}}} \tag{3c}$$

$$\left\langle \frac{\mathrm{d}i}{\mathrm{d}t} \right\rangle = \frac{\varepsilon}{2\pi} \sqrt{\frac{a}{\mu}} \int_0^{2\pi} \cos\theta \sin\beta(\theta)\,\mathrm{d}\theta \tag{3d}$$

Received June 16, 1996; revision received Jan. 16, 1997; accepted for publication Jan. 28, 1997. Copyright © 1997 by the American Institute of Aeronautics and Astronautics, Inc. All rights reserved.

*Reader, Department of Aerospace Engineering.